Vilniaus universiteto
Fizikos fakulteto
Fotonikos ir nanotechnologijų institutas

Aivaras Špokas

ARTIMOSIOS INFRARAUDONOSIOS SRITIES MIKROLAZERIŲ AKTYVIOSIOS TERPĖS TECHNOLOGINIŲ SĄLYGŲ OPTIMIZAVIMAS

Bakalauro studijų baigiamasis darbas

Šviesos technologijų
studijų programa

Studentas Aivaras Špokas

Leista ginti 2024-01-10
Darbo vadovas doc. Renata Butkutė

Instituto direktorius prof. Ramūnas Aleksiejūnas

Vilnius 2024

Vilniaus University
Faculty of Physics
Institute of Photonics and Nanotechnology

Aivaras Špokas

OPTIMIZATION OF TECHNOLOGICAL GROWTH CONDITIONS OF THE ACTIVE REGION FOR NEAR-INFRARED MICROLASERS

Bachelor‘s final Thesis

Light Engineering
Study Programme

Student Aivaras Špokas

Approved 2024-01-10
Academic supervisor Assoc. Prof., Dr. Renata Butkutė

Director of Institute of Photonics and Nanotechnology Prof. Ramūnas Aleksiejūnas

Vilnius 2024

Table of Contents

Abbreviations

AFM – Atomic Force Microscopy

BFM – Beam Flux Monitor

CCD – Charge Coupled Device

CHSH - Conduction, Heavy-hole, Split-off hole, Heavy hole recombination channel

EL – Electroluminescence

FWHM – Full Width at Half Maximum

HH – Heavy Hole

HT – High Temperature

LD – Laser Diode

LED – Light Emitting Diode

LT – Low Temperature

MBE – Molecular Beam Epitaxy

MOVPE - Metalorganic Vapor Phase Epitaxy

MQW – Multiple Quantum Well

NIR – Near-infrared

PL – Photoluminescence

QW – Quantum Well

RHEED – Reflection High Energy Electron Diffraction

RQW – Rectangular Quantum Well

RT – Room Temperature

SQW – Single Quantum Well

TDPL – Temperature Dependent Photoluminescence

TST – Two Substrate Temperature

XRD – X-ray Diffraction

Related Publications

A list of poster presentations and publications related to bismide growth for near-infrared emitters.

Articles in Scientific Journals

1. Monika Jokubauskaitė, Gustas Petrusevičius, Aivaras Špokas, Bronislovas Čechavičius, Evelina Dudutienė, and Renata Butkutė, "Effects of Parabolic Barrier Design for Multiple GaAsBi/AlGaAs Quantum Well Structures," Lithuanian Journal of Physics, vol. 63, no. 4, pp. 264–272, 2023, doi: 10.3952/physics.2023.63.4.8.

Poster presentations

1. Aivaras Špokas, Andrea Zelioli, Evelina Dudutienė, Sandra Stanionytė, Bronislovas Čechavičius, Renata Butkutė, "Optimization of GaAsBi Rectangular QWs for Emission at 1 - 1.2 Micrometre", 25th International PhD student Conference-School "Advanced Materials and Technologies 2023", Palanga, Lithuania, August 21-25, 2023.
2. Aivaras Špokas, Andrea Zelioli, Kipras Mažeika, Augustas Vaitkevičius, Sandra Stanionytė, Aurimas Čerškus, Bronislovas Čechavičius, Evelina Dudutienė, Renata Butkutė, "Development of GaAsBi MQWs technology for NIR emitters", Workshop "Application-oriented material development", Bucharest, Romania, September 12-14, 2023.
3. Aivaras Špokas, Andrea Zelioli, Gustas Petrusevičius, Mikas Paulius Iršėnas, Augustas Vaitkevičius, Sandra Stanionytė, Aurimas Čerškus, Bronislovas Čechavičius, Evelina Dudutienė, Renata Butkutė, "Precise Control of Emission Wavelength in GaAsBi MQW Structures During MBE Growth", 13th PhD Student and Young Researcher conference "FizTech2023", Vilnius, Lithuania, October 18-19, 2023.
4. Aivaras Špokas, Andrea Zelioli, Kipras Mažeika, Augustas Vaitkevičius, Sandra Stanionytė, Aurimas Čerškus, Bronislovas Čechavičius, Evelina Dudutienė, Renata Butkutė, "GaAsBi stačiakampių kvantinių duobių auginimo technologijos optimizavimas artimosios infraraudonosios srities emiteriams" 45th Lithuanian National Physics Conference, Vilnius, Lithaunia, Octrober 25-27, 2023.

1. Introduction

Semiconductors are the foundation of modern electronics, optoelectronics, photonic devices, sensing systems and many more. Ever since the successful production of the first transistor in 1949 semiconductors have been one of the leading research areas in physics and technology. This led to a great understanding of classical semiconductor materials: such as silicon, germanium, or gallium arsenide. Nonetheless, the extensive fundamental and technological research into this field, showed that limitations in achievable emission energies and efficiency of devices are obvious. As a result, the current research is focused on novel alloys and quantum effects occurring in the crystal structure in aims to achieve desired emissions and enhanced device properties.

Near infrared (NIR) is an important region which requires stable and efficient emitters. Its uses span from telecommunications to environmental and biological sensing systems. In 1998 *Oe and Okamoto* [1] were the first to grow a new semiconductor material – GaAsBi, to be used as an active media for NIR laser diodes (LD). Introduction of Bi into GaAs reduces the energy band gap at a high rate of 88meV/% [2]. This reduction is substantially larger comparing with other AIII-BV semiconductor crystals, such as InGaAs or GaAsP. This presents one of the first advantages of GaAsBi, since a lower concentration of Bi is needed it introduces less strain, resulting in less lattice mismatch dislocations, while achieving the same emission. Additionally, GaAsBi has been proposed as a material in which the main cause of optical losses, Auger recombination, can be supressed. Moreover, the spin-orbit split-off energy becomes larger than the energy band gap at Bi concentrations larger than 10% [3]. Finally, GaAsBi based optoelectronic devices have shown stable operation in room temperature [4], making it a great candidate for being integrated into other devices that usually operate in ambient conditions.

Despite all the before mentioned advantages, the growth of GaAsBi is more complicated, when compared to classical materials. Bi has a general tendency to segregate or work as a surfactant. Currently the most suitable growth technique for this material is molecular beam epitaxy (MBE). It allows to achieve the two most important conditions in bismide growth, namely the low substrate temperatures of 420 ˚C and lower, while the precise control of material fluxes allows to achieve an arsenic to gallium ratio close to unity, which is crucial for introduction of Bi. The low temperature growth of GaAsBi is the main limiting factor for successful fabrication of light emitting devices, since the material grows to be highly disordered resulting in more non-radiative recombination. Therefore, the growth must be optimized to achieve the best possible crystalline quality and in turn sufficient optoelectronic properties necessary for laser diodes.

The aim of this work was optimization of the growth conditions for enhancement of emission at 1100 nm from GaAsBi quantum well (QW) structures. Optimization was performed in aims of application of such structures in GaAsBi-based microlasers for a joint Lithuanian – Latvian – Taiwanese research project focusing on NIR sensing applications in reflectance blood oximetry.

The aim was achieved by completing a series of **tasks**:

- To grow a series of GaAsBi RQW test structures for investigation of the dominant growth regime.
- To clarify the influence of temperature and atomic fluxes to the crystallinity and surface morphology of GaAsBi alloy.
- To find optimal growth conditions and main limiting factors and optimize the QWs for emission that is close to 1100 nm (~1.13 eV).
- To grow a bismide based light emitting diode (LED) on AlAs sacrificial layer and measure its optical properties.
- To fabricate a bismide based laser diode (LD) on AlAs sacrificial layer and achieve lasing in the range from 1060 to 1160 nm.

2. Literature Overview

In this subsection, the main properties of GaAsBi are presented, focusing on the optical properties, band gap engineering, growth peculiarities and an overview of the state-of-the-art in bismide light emitting devices and possible application in biological sensing for reflectance blood oximetry.

2.1. Properties of GaAsBi

The wavelength range of 1000-1200 nm has a very well-developed detector ecosystem, though the emitters in this range still require improvements. GaAs platform is the obvious choice for NIR applications since it is well known and cheaper than the alternatives. Lately, bismuth has surfaced as an attractive material for emission energies below the GaAs band gap of 1.42eV due to several properties. First of all, Bi results in a large band gap reduction in GaAsBi. *Francoeur et al.* reported a reduction rate of 88 meV/% in the range from 0 to 3.6% of Bi [2], this value is only surpassed by one other material – GaAsN, where over a 100 meV/% is observed [5]. The main benefit of this is that achieving longer emission wavelength is possible without a large change in the lattice parameter, which means that structures grown on GaAs remain fully strained at the wavelengths longer than 1100 nm and the formation of lattice mismatch dislocations is prevented.

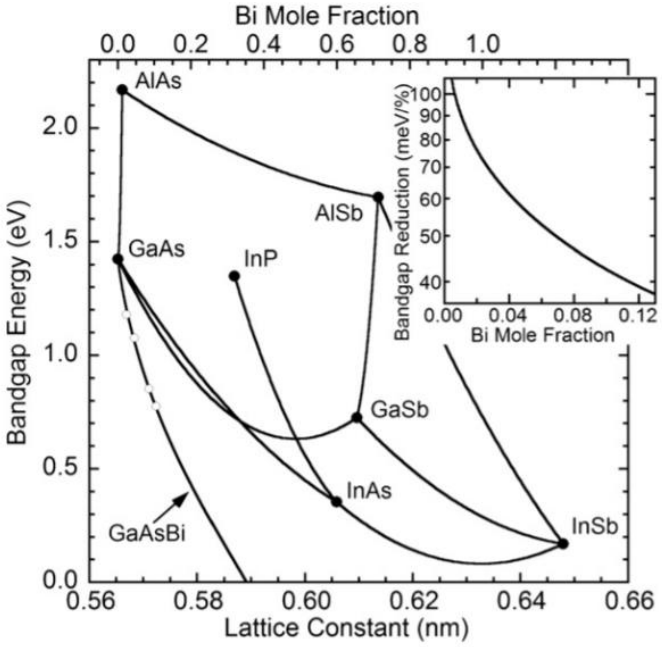

Fig. 1. Energy band gap versus lattice constant for III-V semiconductors. The rate of band gap reduction per Bi mole fraction given in the inset. Taken from [6].

Another motivation for using bismuth was proposed by *Alberi et al.* that was related to the difference in atomic radius of the group V elements in dilute alloys [3]. The Band anticrossing model was first proposed for nitrogen containing alloys, namely InGaAsN [7]. Here N possesses a substantially lower atomic radius then As and highly influences the conduction band. In the case of GaAsBi, Bi with its lower electronegativity and ionization energy influences the valence band.

Experimental results obtained by *Alberi et. Al.* showed that with the introduction of Bi both band gap and spin-orbit splitting Δ_{SO} energies undergo significant bowing and at a certain point of around 10.5 % of Bi content (see Fig. 2.) Δ_{SO} becomes larger than the band gap energy, resulting in a suppression of one of the main non-radiative Auger recombination channels.

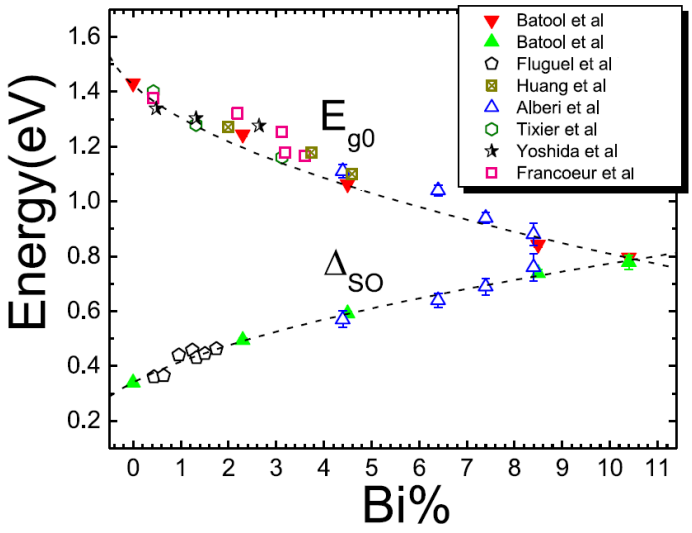

Fig. 2. Change of band gap (E_g) and spin-orbit splitting (Δ_{SO}) energies, with increasing Bi content in GaAsBi at room temperature. Dashed lines represent theoretical modelling, with coloured symbols showing values from structures grown by different groups. Adapted from [8].

A CHSH (conduction, heavy-hole, split-off hole, heavy hole) recombination path becomes supressed (see Fig. 3), due to before mentioned reason. This is a non-radiative recombination path, and it results in reduced efficiencies and threshold currents in NIR laser diodes currently [8]. In a classical case an electron recombines with a heavy hole (hh) but instead of emitting a photon it excites the hh to recombine with an electron in the split off band (CHSH recombination path). Fig. 3. Presents a case where $E_g > \Delta_{SO}$ and the non-radiative recombination is suppressed.

Lastly, GaAsBi shows less band gap sensitivity to temperature. Temperature dependant photoluminescence (TDPL) measurements performed by *Oe and Okamoto*, showed that in a sample with ~2 % Bi PL peak energy shift is only 0.1 meV/K [1]. In addition to that, GaAsBi devices have been demonstrated to work in room temperature [4], making this temperature stability another advantage, when considering device fabrication.

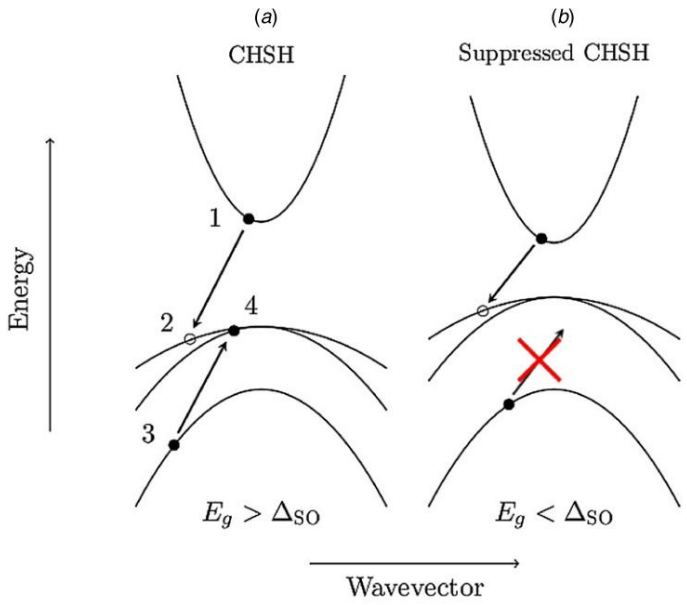

Fig. 3. Band structures for a) CHSH recombination and b) suppressed CHSH Auger recombination. Adapted from [9].

2.2. Growth of GaAsBi

The growth of GaAsBi poses several challenges. They arise from a specific growth window required for Bi introduction, being the low temperature growth and a beam equivalent pressure ratio (BEPR) of As to Ga being close to unity. Despite these challenges in 1998 *Oe and Okamoto* successfully grew a GaAsBi alloy using metal organic vapor phase epitaxy (MOVPE) [1]. Currently, the main growth method for bismides is MBE, with the main advantage of possibility to achieve lower growth temperatures (300 ˚C and below). In this subsection the challenges and peculiarities of bismide growth by MBE are presented.

2.2.1. As:Ga ratio

Both Bi and As are group V elements meaning they compete for the same sites in the crystal lattice, thus a nearly stochiometric As:Ga ratio in necessary for Bi incorporation. A study published by *Richards et al.* pointed to an optimal window of As:Ga ratios in which maximum Bi incorporation is achieved (see Fig. 4.) [10], while *Lewis et al.* provided an experimentally supported model, which points to a saturation value after which lowering the As flux further shows little impact [11]. None the less it must be noted that the latter study did not grow samples at BEPR lower than 0.8.

Furthermore, the control of As:Ga ratio is the dominant factor, when looking at surface morphologies and crystalline quality. With an overpressure of As, GaAsBi is exposed to the As related defects, that were also observed in low temperature (LT) GaAs layers by *Feenstra et al.* [12].

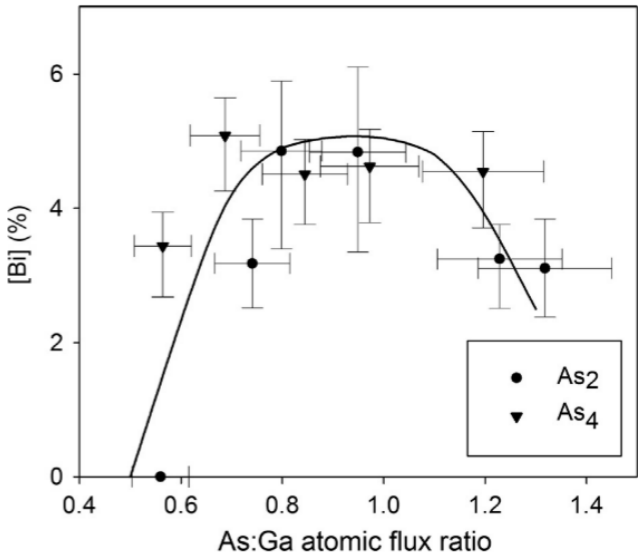

Fig. 4. Bi incorporation dependence on atomic flux ratio of As:Ga (for As_2 – circles, and As_4 – triangles), with tetrameric arsenic fluxes being halved to account for desorption. Taken form [10].

These are mainly As antisite point defects, where in a Ga limited growth As takes a site that should be occupied by a Ga atom. Moreover, As:Ga ratio is also one of the controlling factors for surface droplets. Metallic droplets often form on the surface of GaAsBi samples, if working outside the optimal growth windows. In ratios lower than unity, Ga droplets appear due to the lack of As, in this regime the growth rate would be As limited. At higher As:Ga ratio with a high Bi flux formation of Bi droplets is present. *Puustinen et al*. show a correlation between As:Ga ratio and bismuth incorporation efficiency. Their findings support earlier works with Bi incorporation dropping at As:Ga ratio lower than 1, with surface roughness increasing due to Ga droplets, and Bi droplets appearing at the Ga limited region above a ratio of ~1.17 resulting in reduced smoothness (see Fig. 5) [13].

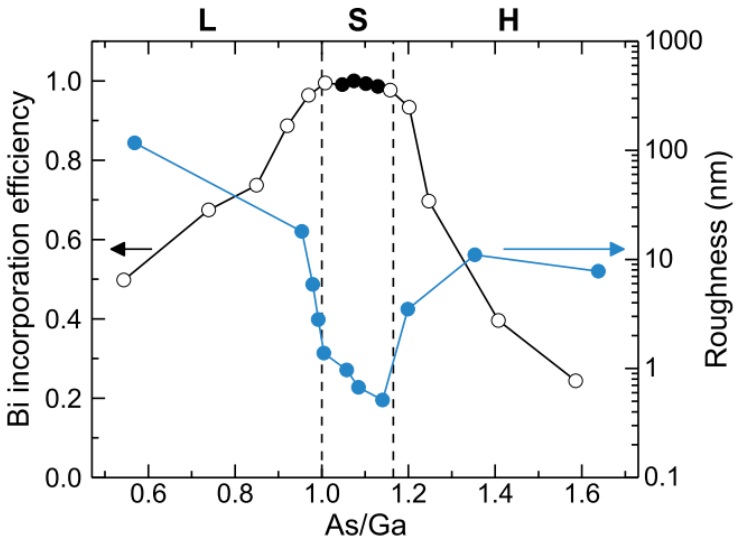

Fig. 5. Bismuth incorporation efficiency and surface roughness for different As:Ga ratios, dashed lines denote the optimal growth window. Taken from [13].

A final type of surface droplets are biphasic Ga-Bi droplets, they appear because of a combination of the two before mentioned regimes. At high Bi:As and low As:Ga ratio. It was also noted by *Carter et al*. that this type of droplet only remains biphasic at liquid form, and they split into Ga and Bi parts post growth [14]. Fig. 6. also points to the fact that maximum Bi contents are achieved in the region where droplet free, Bi and biphasic droplet formation regimes intersect, meaning that an optimal regime is more difficult to achieve, when aiming for a smooth surface and high Bi contents. Nevertheless, it must be noted that measurements of BEPR are individual for every machine due to different geometries (different positions of the sources and beam flux monitor (BFM)). This explains the variation of numerical values between different research groups, though the general tendencies stay consistent. To conclude, As:Ga ratio is one of the key parameters in growing high quality GaAsBi, since in affects both, the band gap via Bi content, and the intensity via defects and surface morphologies.

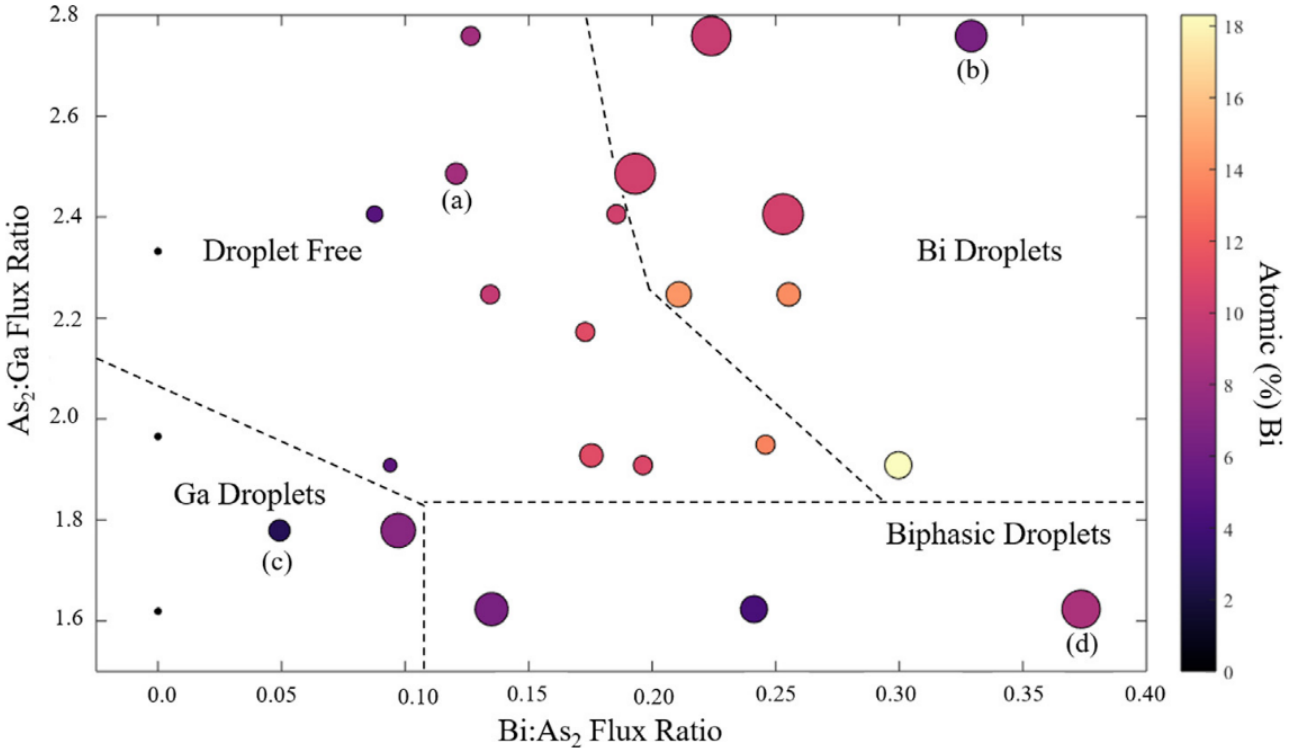

Fig. 6. Surface morphology map for GaAsBi samples grown at varying As:Ga and Bi:As ratios. 4 regions of droplet type are separated by dashed lines. Bi content is colour coded for experimental samples, while the size shows the breadth of the peak. Taken from [14].

2.2.2. Growth Regimes

Bi introduction is one of the main issues in the growth of bismides. Not only does the bismuth itself introduce defects, purely from its nature of being larger than As, but also the low temperature conditions and necessity for very high precision of material flux ratios, introduce more disorder in to the alloy. Nevertheless, exactly temperature and atomic fluxes are the

limiting factors for Bi incorporation as they cover the two growth regimes – temperature and kinetically limited. Temperature limited regime is achieved with a Bi flux that is well in excess of the maximum incorporation value, while As:Ga ratios follow the general rules of bismide growth. *Richards et al.* place the experimentally found limit for Bi incorporation at a growth temperature of ~440 ˚C [10]. Fig. 7. Is a good representation of the temperature limitation, with the use of lower Bi fluxes a saturation line can be seen indicating that Bi incorporation coefficient reaches unity. With an increase of Bi flux the content vs temperature continues to follow a linear trend. The tendency is also shown to be independent of the As species selected.

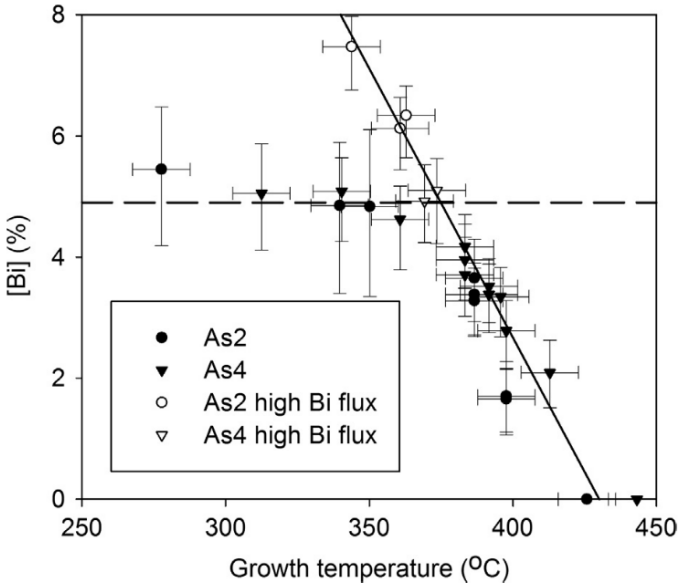

Fig. 7. Bi content vs growth temperature, solid symbols indicate low Bi flux, while black outline symbols indicate high Bi flux. A solid line shows a temperature limited regime, while the dashed line represents a saturation value of maximum Bi incorporation for a given flux.

This linearity is also observed in other works, for example in a publication by *Rockett et al.*, where temperature limited regime is also linear for a series of pin diodes grown at a constantly high Bi flux [15]. Though it must be noted that both of these works showed a difference in the rate of incorporation per a degree of temperature, again pointing to the fact that geometry, and other growth conditions, such as post growth annealing, have influenced the final structures. The later study also looks into the kinetically limited growth, here the temperature is maintained while Bi flux is changed. An observation can be made that at a constant temperature with increasing Bi flux the Bi content is also increased, although this regime is substantially less sensitive, since the fluxes must be increased drastically to achieve higher Bi content. On the other hand, *Ptak et al.* published a deeper investigation into the kinetically limited growth by introducing another parameter – growth rate [16]. Two main conclusions were made. First of them being mainly related to growth rate: the findings show that in this growth regime as the Bi flux is doubled the content also approximately doubles, though when

increasing the growth rate, the Bi content decreases, if flux is kept constant. The second finding observes the surface roughness at different growth rates. Authors attributed the roughness at high and low growth rate to two different reasons. Bi acts as a surfactant, increasing the surface quality, if GaAsBi is grown at low growth rate (160 nm/h) and Bi flux. Increasing the Bi flux results in higher Bi content but the surface smoothness decreases due to droplet formation. This is also a result of Bi on the sample surface, although here the flux is sufficient to have enough Bi on the surface to form droplets. When looking at the high growth rate (960 nm/h) results, the low Bi content provides a worse surface, since here the surfactant effect is too low. By increasing the Bi flux, Bi has a surfactant effect, but not enough Bi for droplet formation. Authors presented results for 640 nm/h growth rate, with a droplet free surface: here for samples up to 8% of Bi the surface remains relatively smooth (see Fig. 8.).

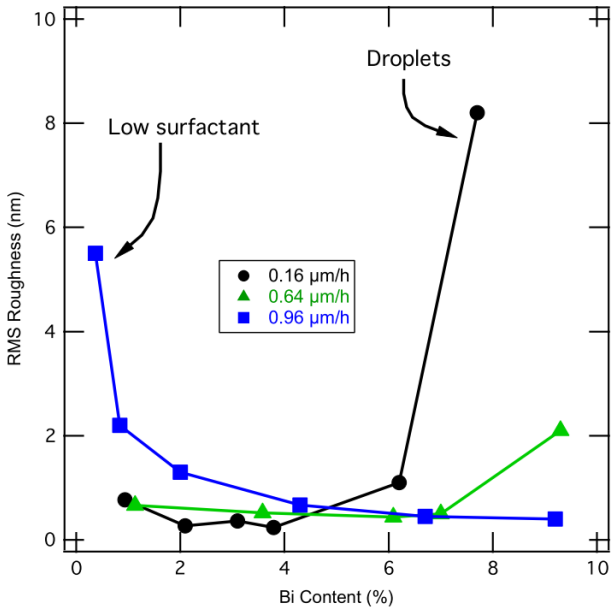

Fig. 8. Surface RMS roughness from AFM scans for samples grown at different growth rate with varying Bi contents. Taken from [16].

2.3. Surface Reconstructions

In-situ surface monitoring is performed for all samples grown with MBE. Reflection high energy electron diffraction (RHEED) is an in-situ surface characterization device that is used to determine growth quality and material composition by gathering information about the crystal lattice from the surface atomic layers. In this subsection surface reconstructions obtained from RHEED will be discussed.

Different semiconductor alloys have their inherent reconstructions that can be monitored during growth. Surface reconstructions depend on the growth temperature, material fluxes and material

composition. Thus, it can be used as a tool of confirming Bi incorporation or determining the growth window. *Masnadi-Sahirai et al.* published and in-depth surface reconstruction investigation for GaAsBi and GaAs grown at low temperatures and low As:Ga ratios (see Fig. 9) [17]. GaAs has well known surface reconstructions, starting from (1x1) bulk reconstruction, which is indicative of a stochiometric As:Ga ratio, while (2x4) is a sign of high quality GaAs grown at high temperatures, when the limiting flux is Ga. (1x3) is the reconstruction attributed with low temperature GaAs growth, whit a transitional reconstruction of (2x3) from high temperature regime. Finally, (3x1) and (4x1) are seen in Ga-rich growth, where a further reduction in As:Ga ratio would result in Ga droplet formation and a surface that cannot provide any reconstructions. Growth of GaAsBi is only possible at specific conditions, exactly in the region where the conditions are met, a difference from GaAs reconstructions is observed (see Fig. 9). A (2x1) reconstruction observed at temperatures under 400 ˚C and a stochiometric As:Ga ratio is an indication of GaAsBi growth, with the (2x3) reconstruction that is proposed to be a transitional region between (2x1) and (1x3) reconstructions, and can be explained by the non-uniformity of As flux, where growth of bismides can still be achieved. Finally, it can also be noted that usually reconstructions during bismide growth are way less pronounced and look out of focus, this can be explained by both the disordered material and Bi surfactant properties.

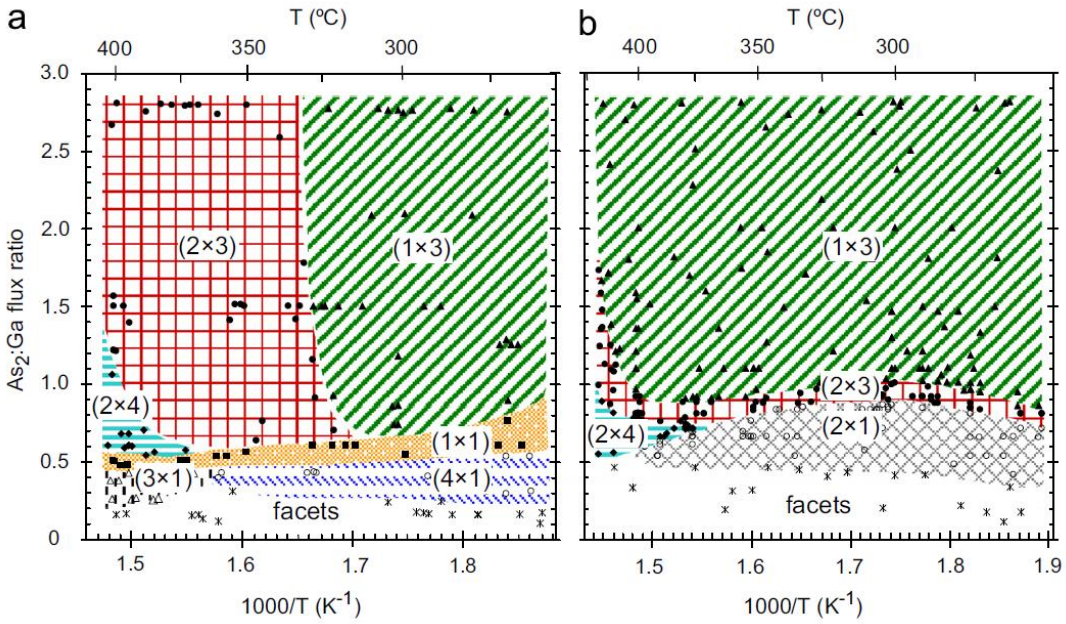

Fig. 9. Surface reconstructions of a) GaAs, b) GaAsBi at low temperatures (<450 ˚C) and As:Ga ratios lower than 2.82. Taken from [17].

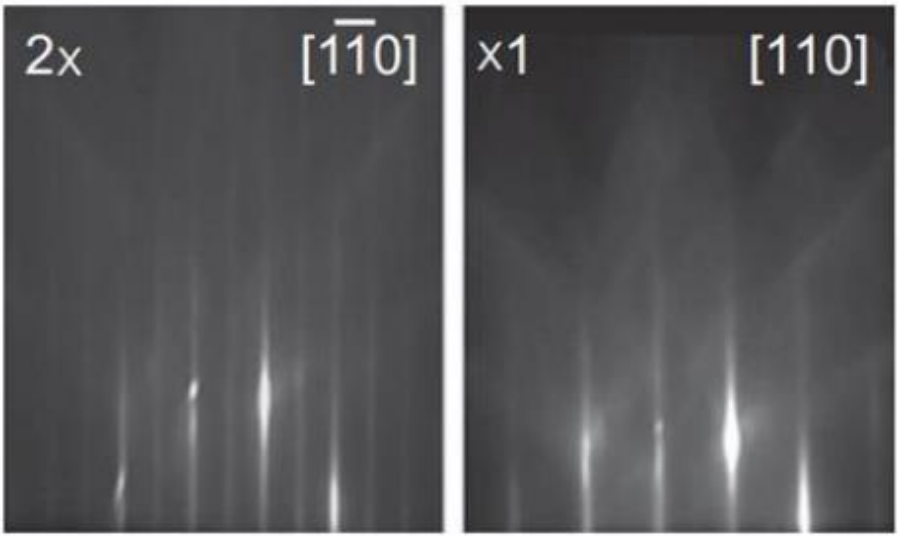

Fig. 10. (2x1) surface reconstruction of GaAsBi. Taken from [17].

2.4. Quantum Wells

The emission wavelength of GaAsBi QW samples can be controlled by two parameters. First, the thickness is a defining factor, as the QW shrinks the states in the well are pushed up, increasing the distance between bands, resulting in higher emission energies. Second factor is the composition of the alloy. As it was explained in section 2.1 Bi is used to bring the bands closer in the GaAs platform. Analogical process happens in the QWs as well. The inherent result from growing QWs is an increased band gap energy, though the introduction of Bi still shifts the emission deeper into the IR. None the less, use of QWs in mismatched structures helps with reducing the stain, and maintaining fully strained crystals, whilst it has also been seen that lasing is easier to achieve in QW laser diodes.

2.5. GaAsBi Light emitting devices

The most popular emission wavelength for NIR laser diodes has been 1550 nm, since it represents the telecommunications window that is currently in use for fiber optical connection. Nonetheless, shorter wavelengths also find their uses mostly in sensing applications for highly selective environmental gas sensing or integration in wearable tech for blood oxygen sensors. Despite the before mentioned difficulties in growing GaAsBi layers, many groups successfully produced GaAsBi light emitting devices [4, 18-21]. In this subsection the history and the current state-of-the-art for bismide devices will be overviewed.

The first GaAsBi LED was produced by *Lewis et al.* in 2009. Room temperature electroluminescence (RTEL) was achieved at a peak wavelength of 987 nm from a 50 nm thick GaAsBi layer with 1.8% of Bi [18]. The pin structure was realised using MBE at the substrate temperature of 300 ˚C for the bismide and GaAs spacer layers. Another notable LED structure

was grown by *Patil et al.* Since GaAsBi must be grown at low temperatures, this also hinders the quality of the barriers, when considering a MQW (multiple quantum-well) structure. A way to retain good crystalline quality of the barrier was realised by performing TST (two substrate temperature) growth [20]. The 11-period structure, with GaAsBi layers grown at 350 ˚C and barriers at 550 ˚C, yielded an impressive 1230 nm peak wavelength, with 4 % of Bi content in the QWs.

Tominaga et al. [4] was the first to achieve lasing from GaAsBi active area. A photo-pumped structure with 2.5% Bi thick layer grown by MBE, exhibited lasing at 982.8 nm. Authors also reported the before mentioned low temperature dependence of the emission wavelength. A further notable device was fabricated by *Ludewig et al.* 3 years later. It was the first electrically pumped single quantum well (SQW) laser diode utilizing a GaAsBi active region [19]. Their 2.2 % of Bi content 6.4 nm thick GaAsBi SQW sandwiched between $Al_{20}Ga_{80}As$ barriers achieved room temperature lasing at 947 nm, by electrical pumping. Their proposed design is still maintained to this day with doped AlGaAs cladding layers for waveguiding and charge transfer, between dopped GaAs layers on top and bottom of the structure, to reduce resistivity for contact layers. Nonetheless, the search for longer wavelengths continued and the record-breaking emission was demonstrated by *Liu et al.* [21]. The group showed lasing at 1276 and 1407 nm from a 5.8% of [Bi] optically pumped microdisk laser with a disk diameter of 750 nm. Authors also showed that with larger disk diameters shorter emission wavelengths are achieved and the lasing power threshold becomes larger.

2.6. NIR Radiation for Blood Oxygen Sensors

NIR light emitters have long been used in pulse oximetry. Many small form wearable devices provide a non-invasive method for blood oxygen detection using two wavelengths 660 nm and 940 nm [22]. The detection hinges on the difference in absorption for oxyhaemoglobin, which absorbs for of the NIR wavelength and non-oxygenated haemoglobin, which absorbs more of the red light. A problem appears with measurements through a thicker layer of tissue where reflectance mode pulse oximeters are used. Here inaccuracy originates from the different penetration depth of the two wavelengths. Therefore, a suggestion is made to produce a double wavelength laser-based pulse oximeter emitting at 800 nm and 1100 nm. In this range the absorption from haemoglobin also differs considerably, in addition to having an almost identical penetration depth into soft tissues.

3. Methods

3.1. Molecular Beam Epitaxy

All structures presented in this work were grown using Veeco GENxplor R&D MBE system. This MBE equipment consists out of 3 main parts: (i) a load-lock chamber used for sample introduction/extraction and initial degassing sequence, (ii) a buffer chamber for further oxide removal, (iii) growth reactor, where final deoxidation is performed and growth procedure is carried out.

The growth reactor houses 10 material source cells, called pseudo-Knudsen cells (k-cells). 7 of them were used in this work, containing high purity (7N5) metallic materials, namely bismuth gallium, aluminium, and arsenic, in addition to silicon and beryllium, which are used for doping. Two separate Ga cells, calibrated for different fluxes, were used to achieve different Al contents, while growing AlGaAs. All sources have a two-zone heating configuration for bulk and tip. The As source in this system has a special design. It is equipped with a cracker that splits As tetramers (As_4) into dimmers (As_2) by the cracker heating being set at 900 ˚C. It also has a variable diameter valve that allows for a precise As flux control, that is crucial for bismide growth. The valve allows to quickly change the As flux between growth of two subsequent layers e.g. GaAsBi and LT GaAs. Furthermore, the growth reactor has a rotating substrate holder, where the rotation ensures a homogeneous coverage of the substrate, and the rotation speed is variable. Directly atop of the substrate holder is the substrate heater. The temperature of it is monitored via a thermocouple. Finally, the reactor is also equipped with *in-situ* characterization devices: RHEED for growth rate measurement and observation of surface reconstructions; and band edge thermometry “BandiT” system, for accurate substrate temperature measurement (see subsection 3.2.)

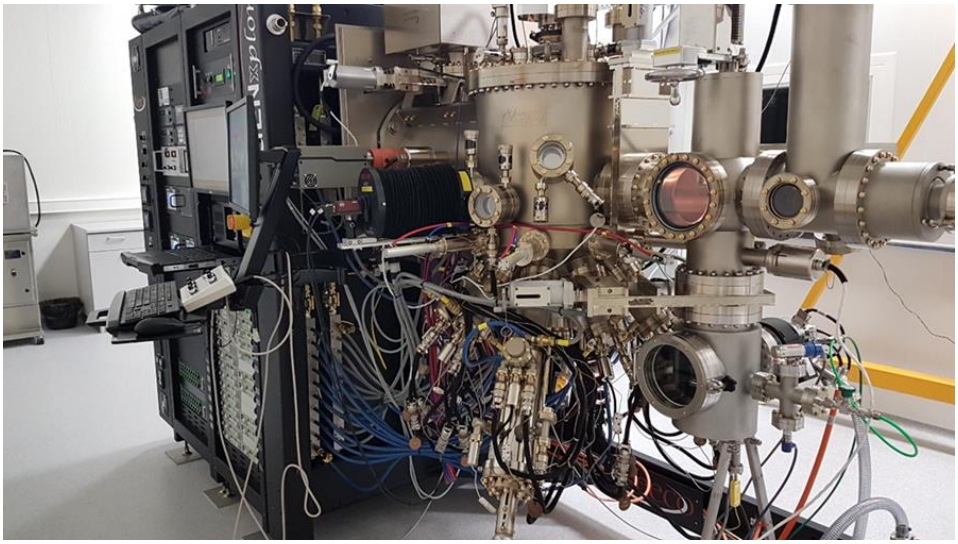

Fig. 11. *Veeco GENxplor R&D* solid-state MBE system. FTMC, Vilnius.

A crucial parameter for an MBE system is the background pressure. Extreme vacuum conditions are maintained for two main reasons. First, the background elements can be deposited on to the substrate, ruining their crystal quality, and consequently, lowering the emission intensity from light emitting structures. Second, the molecular mean free path is inversely proportional to the partial pressure. In MBE growth the mean free path is in the order of meters ensuring that the material reaches the substrate. The low pressure is ensured in two ways, first of them being a series of pumps (rotary, turbomolecular, ion and cryopump) that regulate the pressure in all three parts of the system. Secondly, the growth reactor is also cryopanelled. Liquid nitrogen is supplied into the walls on the growth chamber, as a result, when the elements reach the walls, they are deposited on them, further helping to control the background vacuum. All these measures ensure pressure in the order of ~10^{-10} - 10^{-11} Torr before growth and around 10^{-8} Torr during growth. Usual pressure in the load-lock and buffer chambers is in the order of 10^{-7} - 10^{-9} Torr.

All growth parameters are controlled via a manufacturer provided computer software. The material fluxes are changed by varying the temperature of k-cells, while other parameters have direct inputs. The software also allows to create growth recipes, from which the equipment automatically opens/closes sources, adjusts temperatures and valve position.

3.1.1. Substrate Preparation

All the samples were grown on epi-ready GaAs (100) substrates. As the substrate is loaded into the load lock chamber it is heated for 2 hours at 200 ˚C starting the oxide removal process, secondly it is further heated for an hour in the buffer chamber at 300 ˚C before the last step of heating it to 700 ˚C or higher in the growth chamber for ~15 minutes with maximum arsenic flux supplied. The oxide removal is observed using RHEED, where image of a deoxidized substrate provides longer streaks with higher contrast. Additionally, oxide removal increases the pressure in the growth chamber, thus no increase in pressure after further heating signifies successful deoxidation.

3.2. In-situ Characterization

3.2.1. Reflection High Energy Electron Diffraction

Reflection high energy electron diffraction (RHEED) is a standard in-situ characterization device mounted on almost every modern MBE system. It consists of two main parts: the electron gun, and a detection system (phosphor screen and CCD chip). The electron beam grazes the sample at a small angle (1-3˚), the diffracted beam is then directed to the phosphor screen, where electrons are converted into a visible picture, that is captured by a CCD chip. RHEED is utilized in two ways, growth rate measurement and reconstruction monitoring. Our

system is equipped with a “k-Space Associates 400” RHEED system, shown in Fig. 12.

RHEED has a shallow penetration depth of only up to 3 monolayers, thus it provides information on the surface of the sample. A signal of epitaxial growth is a streaky RHEED pattern, which is known as reconstructions. Reconstructions can be used as an identification for different alloy growth conditions or compositions. As explained in section 2.4., GaAs has varying surface reconstructions depending on material flux ratios or growth temperature, while reconstructions shown in Fig. 10 are indicative of bismide growth. Observing these reconstructions gives instant feedback and can immediately point to a mistake in growth recipes or signal a rapid lowering of a material flux when a source becomes empty.

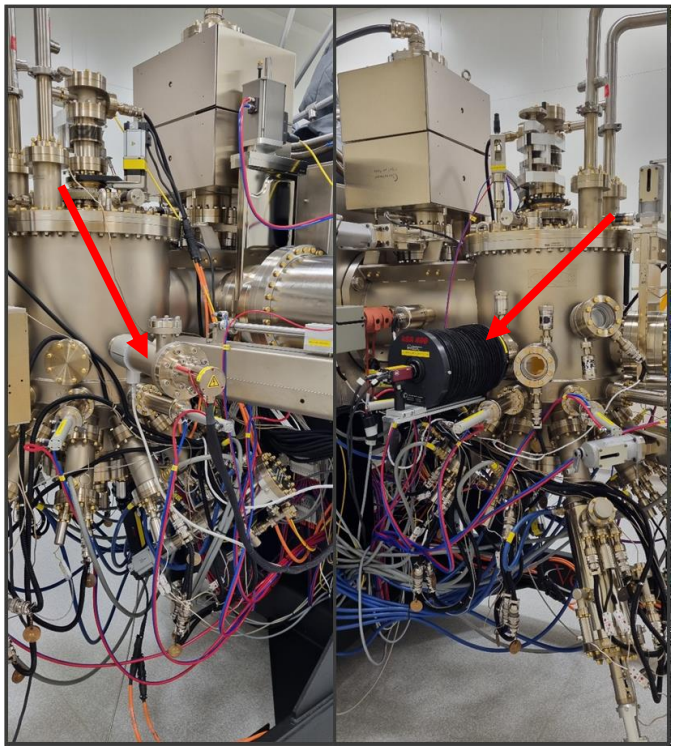

Fig. 12. “kSA RHEED 400” system. Electron gun on the left, detector/CCD on the right (pointed out by red arrows), mounted on *Veeco GENxplor R&D* MBE system’s growth reactor.

Second application of RHEED is growth rate measurement. Growth rate is one of the vital parameters in MBE growth. Not only can it affect the Bi incorporation and surface quality of grown bismide alloys (see section 2.2.3.), but it is also the way for growth time calculations, when aiming for a specific thickness of epitaxial layers. Growth rate is estimated from RHEED intensity oscillations and is made possible by the fact that the RHEED intensity is directly linked to the smoothness of the topmost atomic layers.

If the surface is filled by a complete atomic layer the RHEED intensity is observed at a maximum. When around half of a new atomic layer form, the surface smoothness is the worst, thus resulting in a RHEED intensity minimum. As islands on the surface connect with each other, the surface gradually smoothens before reaching a new maximum. Consequently, the time that passes between two maxima is the time it takes to grow a full monolayer. If the lattice parameters of a grown alloy are known, growth rate can be recalculated for nanometres.

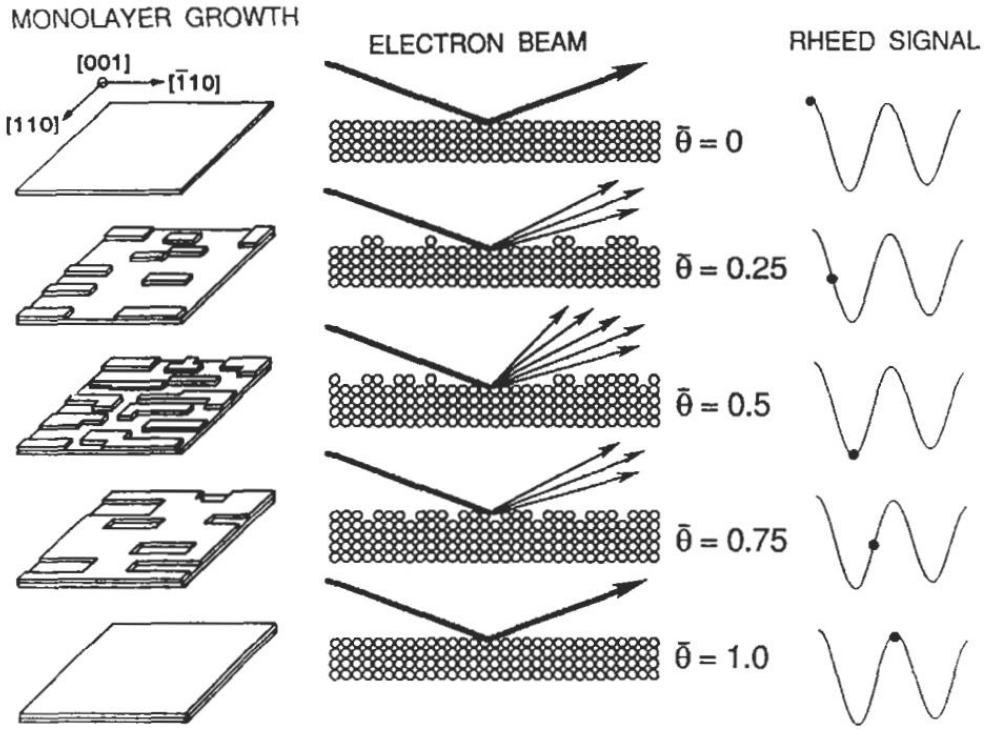

Fig. 13. RHEED intensity oscillation dependence on surface smoothness. Taken from [23].

3.2.2. Band Edge Thermometry

Another in-situ characterization device is used for substrate temperature measurement. As explained in section 2.2.3. Temperature can be the limiting factor in Bi incorporation, thus accurate temperature monitoring is crucial. “k-Space Associates BandiT” is a thermometry tool mounted onto an MBE system for real time temperature readings. It uses the semiconductor band gap vs temperature dependence to provide temperature reading by measuring the absorption edge. The measurement can be conducted in two ways, one being the reflection mode, where an external light source is used to illuminate the substrate and the diffusely scattered light is then detected. This configuration requires a heated view port, since the spectra of the external light source is viewport coating sensitive and could not be used in this work due to a malfunction in the viewport itself. A second configuration, that is suitable for narrower band gap materials such as GaAs is IR transmission mode. Here the absorption

edge is also estimated, but no additional light source is needed, resulting in minimal modifications to the growth reactor and mitigating the necessity for a heated viewport. The substrates used in this work were GaAs. This material is transparent to most of IR, thus in this configuration the heater doubles as an IR light source. The part of the light transmitted through the substrate changes with the temperature, thus a reading can be produced. A configuration provided by the manufacturer ("Wafer Technology Ltd.") of the substrate was used, since the measurement is sensitive to dimension, doping concentration and polishing type.

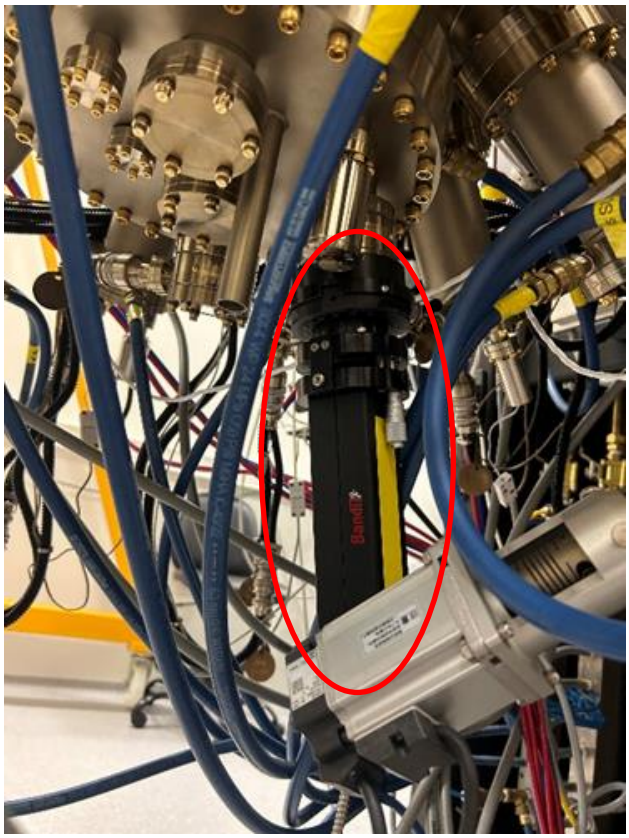

Fig. 14. "kSA BandiT" detector (circled in red), mounted on the bottom of *Veeco GENxplor R&D* MBE system's growth reactor.

3.3. Luminescence Measurement

3.3.1. Photoluminescence Measurement

Photoluminescence (PL) is a measurement used to investigate the band gap of a material by investigating the electron and hole transitions in a semiconductor material. It is a simple to use and usually non-destructive method that provides the quickest possible feedback for the growth sessions. The PL measurement is conducted by exciting a sample with a light source (usually a laser), that emits photons of higher energy than the band gap of the investigated material. The higher energy photons excite electrons in the valence band. As a result, they are elevated to a higher state in the conduction band. Then this electron non-radiatively gives away energy to fall to the lowest possible state in the conduction band from where, in the case

of direct band gap semiconductors, it radiatively recombines with a hole from the valance band. This recombination emits a photon that is of comparable energy to the energy band gap of the material. In addition, since the energy band gap shift with Bi content is known, modelling was made for the structures grown in this work, thus the Bi content can be estimated from the PL measurements. Moreover, one can also look at the intensity of the PL spectra, which can reveal information on the crystalline quality of grown structures. As more defects are present, they induce more non-radiative recombination centers. As a result, less band-to-band transitions happen resulting in a drop of PL intensity.

Room temperature PL (RTPL) measurements were performed as the main characterization tool, providing instant feedback for the upcoming growth sessions. A 532 nm wavelength diode pumped solid-state (DPSS) laser was used for excitation, at an constant intensity of ~5 kW/cm^2. The PL signal from the sample was divided into spectral components with a step of 1 meV via a monochromator and registered using a thermoelectrically cooled InGaAs photodetector. A lock-in amplifier was used for signal amplification. It is crucial to note that the RTPL set-up and its experimental conditions are kept constant between all measurements, thus all the spectra are comparable.

3.3.2. Electroluminescence Measurement

Two electroluminescence (EL) set-ups were used to investigate device performance. These structures were grown with thick doped p and n type regions. Thus, PL measurements were not carried out, since the excitation does not reach the intrinsic layers that should act as device active regions. Consequently, to investigate the band gap properties of *pin* structures indium contacts were placed on the n and p type GaAs layers to perform EL measurement. Similarly to PL, electroluminescence also achieves radiative recombination from band to band transitions of electrons and holes. Only here, the recombination is caused by the electric field. The holes and electrons are separated by doping and recombine, when a current through the sample is applied. For room temperature EL (RTEL) the exact same conditions were used, except for the type of excitation, while for temperature dependent EL (TDEL) temperatures of down to 30 K were achieved using a cryostat cooled by liquid helium, with excitation from an electrical direct current power supply. The RTEL setup can also be modified to record lasing, though in pumping of an LD a pulsed bias is applied at 1 kHz repetition rate of 15 to 200 ns pulses.

XRD measurements were used to verify the thicknesses and Bi contents in some of the grown structures. Additionally, AFM was used to investigate the surface quality.

4. Results and Discussions

A series of around 150 samples in total were grown during the investigations related to this work. The majority them were GaAsBi RQW test structures, grown in aims to achieve optimal conditions for applications in emitting devices (see subsections 4.2. and 4.3.). Furthermore, calibration samples for doped layers and devices were also grown and are discussed in subsections 4.4. and 4.5.

4.1. Sample Growth

Multiple GaAsBi QW samples were grown under various growth conditions in aims to optimize the growth procedures and achieve better control of emission energy with enhanced reproducibility. The investigation was split into two parts: (i) influence of atomic flux related conditions, and (ii) influence of temperature related growth conditions. The shape of the QW was selected to be standard – rectangular, and the number of QWs was selected to be 3 or 5. Majority of the grown structures were capped with high temperature GaAs (~580 ˚C) in aims to mimic the device fabrication procedures, where doped regions are grown at higher temperatures, than the active region. Prior the growth standard preparation procedures were carried out: full deoxidizing cycles, and flux calibrations. The investigatory part of MQW test structures helped to determine the optimal growth conditions for device fabrication. Technological parameters are given as follows: (i) material fluxes are measured with a beam flux monitor before each growth session, (ii) flux ratios are given as BERP obtained from subsequent measurements, (iii) temperatures are measured via “BandiT” band edge thermometry tool.

4.2. Influence of Atomic Fluxes

A series of 9 samples were grown to investigate the impact of As:Ga ratio and Bi flux. Three different As:Ga ratios and three different Bi source temperatures were selected, while trying to keep the other growth parameters constant (see Table 1). All structures contained five 5.5 nm thick GaAsBi RQWs capped with HT GaAs. Grown at a constant growth rate of 540 nm/h (note that the growth rate is given for GaAs and is adjusted using a constant multiplier for GaAsBi).

These structures can be split into 6 sets of three samples with either an identical Bi flux or As:Ga BEPR. In the first set of samples, VGA1377, VGA1378, VGA1379, the outlying emission (VGA1377) can be explained by the influence of temperature, caused by inaccurate calibration (see Fig. 15).

Table 1. Main technological growth and optical measurement parameters. Sample number, growth temperature of the bismide layers (T Growth), PL peak position (Ep) and intensity (Ip), bismuth source temperature (Bi base), As:Ga BEPR, an Bi pressure (Bi P).

Sample	*T Growth (°C)*	*E_p (eV)*	*I_p (arb. u.)*	*T Bi (°C)*	*As:Ga BEPR*	*P Bi (Torr 10^{-7})*
VGA1377	332	1.07	13	500	1.06	1.43
VGA1378	351	1.15	25	520	1.06	2.55
VGA1379	350	1.15	60	530	1.06	3.35
VGA1381	350	1.13	46	520	1.21	2.55
VGA1382	350	1.10	39	530	1.21	3.35
VGA1383	350	1.12	56	500	1.21	1.43
VGA1384	350	1.11	44	530	0.85	3.35
VGA1385	350	1.17	14	520	0.85	2.55
VGA1386	360	1.09	61	500	0.85	1.43

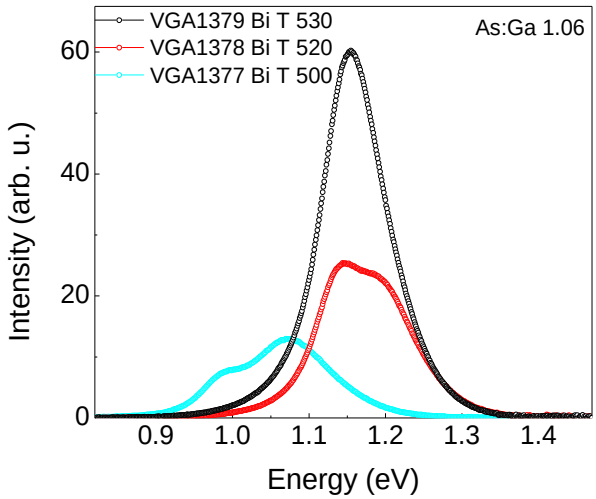

Fig. 15. RTPL spectra for GaAsBi 5xRQW samples grown at varying Bi flux (T Bi 500 - 530 ˚C) and constat As:Ga BEPR (1.06).

Two out of three samples possess asymmetrical, double peak spectra that is attributed to either a non-uniform thickness or Bi content between the MQWs (reasons discussed in more detail in subsection 4.3.). Nonetheless, sample VGA1379 shows interesting results. Its peak intensity is more than double that of the other two structures, and the overall shape of the spectra is more symmetrical with one pronounced peak. This could be attributed to the high amount of surface Bi which acts as a surfactant as explained in subsection 2.2.2. The surfactant properties result in an increased surface smoothness, additionally it helps with Bi incorporation, thus a higher intensity and more symmetrical emission spectra is achieved.

Furthermore, when looking at the overall impact of Bi flux it seemed to have no correlation with emission energies of the grown samples. Even though a fluctuation of around 0.1 eV can be

observed in the whole set, they look to be independent of the flux, meaning that higher Bi flux does not ensure larger Bi content in the structure in the growth window that was used in this work.

Investigation of As:Ga ratio in the range from 0.85 to 1.21 shows no impact to emissions is yet again. For samples grown at a low 0.85 As:Ga BEPR, it was supposed that, due to the appearance of more free group V sites, caused by the lack of As, more Bi could be incorporated into the structures. Though, this is seen to not be the case, while in the set of samples grown at Bi source temperature of 520 ˚C (VGA1385), it even exhibited the highest emission energy, pointing to the low Bi content, Furthermore the spectra turned out to be wide, with multiple peaks and low intensity, pointing to bad crystalline quality and homogeneity of the QWs (see Fig. 16).

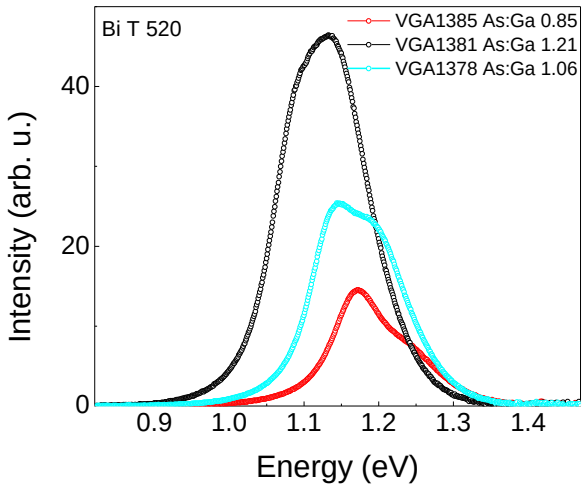

Fig. 16. RTPL spectra for GaAsBi 5xRQW samples grown at constat Bi flux and varying As:Ga BEPR.

The obtained results show relations to the findings published by other groups. The As:Ga BEPR investigation matches the publications by *Richards et al.* [10], and *Puustinen et al.* [13], where an interval of As:Ga ratios was found, where Bi incorporation saturates at a maximum and quickly drops with either an increase or a decrease of this ratio (see Fig. 4 and Fig. 5). When considering Bi flux, it is shown by several groups that it can be used as a controlling factor for emissions. Nonetheless, it must be noted that the Bi fluxes used in the works of *Ptak et al. and Rockett et al.* [15, 16] were smaller by orders of magnitude. In our case we can state that all Bi flux values were above the saturation point of maximum incorporation for the selected growth rate and growth temperature. Finally, a different Bi flux showed the best result (highest flux for 1.06 ratio and lowest for 0.85 ratio), thus it shows that optimal conditions are a combination of the two parameters, where for each ratio an optimal flux must be found.

4.3. Influence of Temperature

In this subsection the tendencies and phenomena seen on the grown samples related to the growth temperature are reviewed. In the earlier work related with substrate temperature measurement and

calibration using “BandiT” it was noticed that using thermocouple readings provides little correlation between temperature and emission energies, while samples grown at matching band edge temperatures showed decent reproducibility. The structures chosen for this part were 5.5 nm thick GaAsBi 3xRQW structures, capped with low temperature GaAs (matching temperature to bismide layers). Such recipe was chosen to eliminate the double peak nature of the PL seen in HT capped samples. Furthermore, the lower number of QWs allowed for more stability in the homogeneity of the QWs. Finally, a temperature limited growth was achieved in the same growth window, which supports the results discussed in the subsection 4.2. and presented two linear temperature dependent coefficients of a band gap shift of 3.5 meV/˚C and bismuth content relation of 0.071 %Bi/˚C (see Fig. 17). Such linear tendency is also in agreement with *Richards et al.* [10] (see Fig. 7).

Table 2. Main technological growth and optical measurement parameters for samples grown in the temperature limited regime. Sample number, growth temperature of the bismide layers (T Growth), thermocouple temperature, PL peak position (Ep) and intensity (Ip), As:Ga ratio, and Bi pressure (P Bi).

Sample	*T Growth (°C)*	*T Thermocouple (°C)*	*E_p (eV)*	*I_p (arb. U.)*	*As:Ga BEPR*	*P Bi (Torr 10^{-7})*
VGA1353	335	426	1.03	25.0	1.03	1.89
VGA1388	305	375	0.94	0.7	1.03	1.90
VGA1389	365	460	1.15	11.4	1.03	1.90

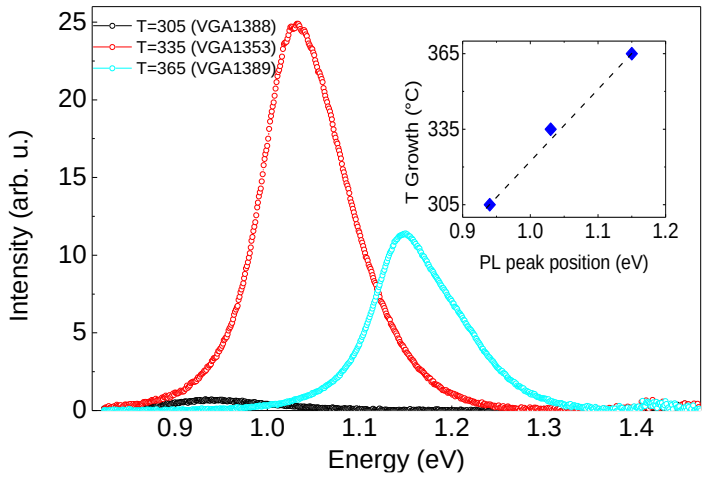

Fig. 17. PL spectra comparison for 3 different GaAsBi 3xRQW samples grown at different substrate temperatures, PL emission energy dependence on substrate temperature provided in the inset (line serves as eye guide).

Consequently, the investigation was continued with HT capped structures as a final calibration step for device growth, where temperature increase after the growth of the intrinsic region is

unavoidable. When considering HT capped samples both the bismide layer temperature and the capping layer temperature were calibrated pre-growth. Meaning that the empty substrate temperature is taken through the heating and cooling cycles, with matching start and end points. For this series the target temperatures were 335 ˚C for bismide layers and 575 ˚C for HT cap. The samples were grown at matching Bi source temperature of 510 ˚C and an As:Ga ratio in the interval of 1.02-1.04, other important parameters are given in Table 3.

Table 3. Optical and technological parameters for samples grown at matching temperature, Bi flux and As:Ga ratio. Sample number, PL primary peak position (E_{p1}) and intensity (I_{p1}), PL secondary peak position (E_{p2}) and intensity (I_{p2}), temperature ramp rate for heating (RR up), and for cooling (RR down).

Sample	*E_{p1} (eV)*	*I_{p1} (arb. u.)*	*E_{p2} (eV)*	*I_{p2} (arb. u.)*	*RR up*	*RR down*
VGA1367	1.075	29	-	-	50	50
VGA1369	1.082	62	-	-	50	50
VGA1370	1.000	17	1.120	7	25	25
VGA1371	1.080	43	-	-	5	5
VGA1372	1.137	34	1.200	17	25	25
VGA1373	1.070	36	-	-	5	25
VGA1376	1.097	84	-	-	25	5

From the table it is seen that for samples with a single PL peak (VGA1367, VGA1369, VGA1371, VGA1373) high reproducibility of the results was achieved with the largest difference in emissions being only 12 meV. The stability of emission wavelength was increased, when compared to LT capped samples presented in earlier works, where the maximum difference in a series of 4 samples was 25 meV. Such behaviour can be attributed to the fact that here the growth of HT cap acts as an annealing of the sample. The HT growth is well in excess of the 440 ˚C, which was shown to be the limit of Bi incorporation by *Richards et al.* [10] Consequently, it can be suggested that this annealing results in higher Bi segregation. Thus, when the structure is both grown and annealed at identical temperatures, bismide layer growth temperature calibration inaccuracy can be compensated with a more accurately calibrated cap temperature.

Nonetheless, this annealing presents an additional problem – the multiple peak nature of the PL. In an earlier work we have already shown the direct relationship between cap temperature and emissions for pairs of single quantum well (SQW) samples grown at exactly matching conditions except for cap temperature (see Fig. 18).

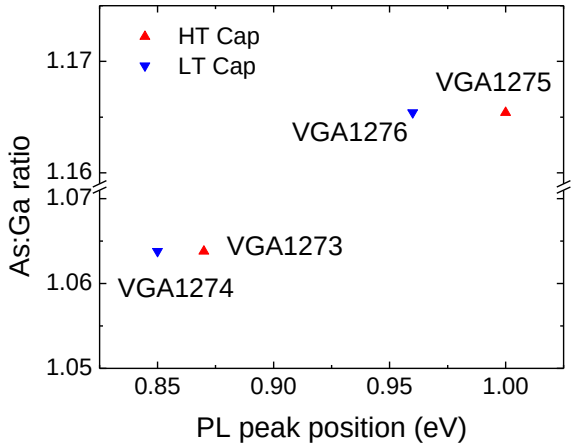

Fig. 18. Comparison of PL peak position for pairs of high and low temperature capped samples, grown under the same conditions (VGA1274 and VGA1273 with As:Ga ratio 1.0638 and 525 °C Bi source; VGA1276 and VGA1275 with As:Ga ratio 1.1654 and 525 °C Bi source).

The change in emission can be explained by the change in Bi content due to segregation and the subsequent multiple peaks are a sign of several QWs containing different amounts of Bi. A hypothesis was raised that the different QWs are a result of them being grown at slightly different temperatures, since it was noticed that with a high ramping rate of the heater, it would take a very long time (20 min or more) for the temperature measured on the substrate to stabilize. Therefore, a series of samples with varying temperature ramping rates of 25 ˚C/min and 5 ˚C/min were grown (default ramping rate - 50 ˚C/min if not specified). Two reference samples were grown with a ramp rate of 25 for both cooling and heating, with both of them having multiple peaks (VGA1370, VGA1372) (see Fig. 19). Three samples were grown with either both cycles done at ramp 5 (VGA1371) (see Fig. 20) or one of the cycles at ramp 5 and other at ramp 25 (VGA1373, VGA1376) (see Table 3, and Fig 21).

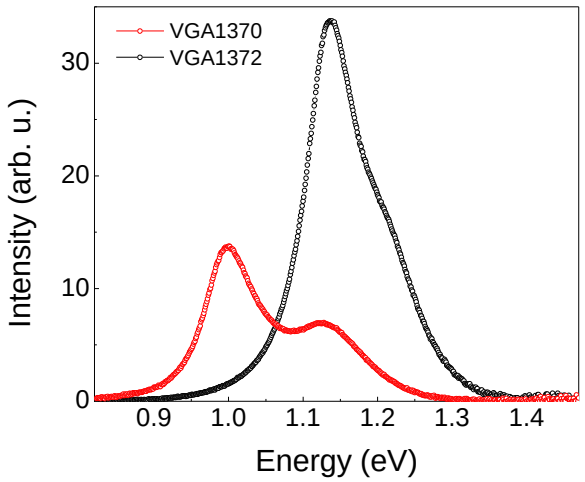

Fig. 19. RTPL spectra for samples grown at temperature ramping rate of 25 ˚C/min for cooling and heating.

When comparing Fig. 19 and 20 it is seen that the sample grown at a low ramping rate exhibits a more symmetrical RTPL spectrum with a singular pronounced peak at a higher intensity, partially confirming the hypothesis that ramping rates can help to eliminate secondary peaks. Though, such growth is quite inefficient from the technological standpoint, since the temperature change steps took 90 min out of the total 113 min growth procedure, thus two intermediate growth recipes were tested (see Fig. 21).

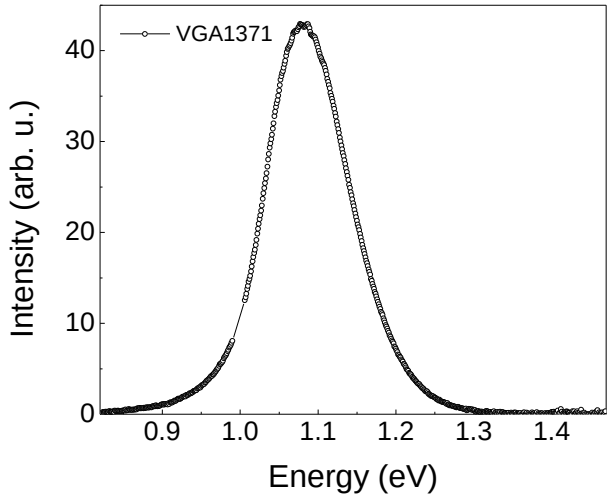

Fig. 20. RTPL spectrum of a sample grown at temperature ramping rate of 5 ˚C/min for cooling and heating. (break in the spectra is a measurement artefact).

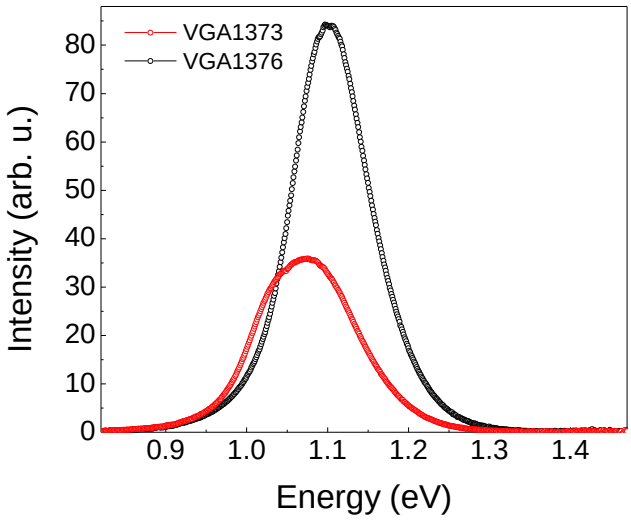

Fig. 21. RTPL spectra for samples grown at varying temperature ramping rates. VGA1373 (red) 25 ˚C/min cooling and 5 ˚C/min heating, VGA1376 (black) 5 ˚C/min cooling and 25 ˚C/min heating.

The spectra in this case look quite different, while VGA1373 has a larger full width at half maximum (FWHM) and looks to have two peaks, the VGA1376 is quite symmetrical and has the best FWHM of 117 meV out of the whole set. The low ramping rate, when cooling ensures enough time for the temperature of the bismide layers to stabilize, thus all of the QWs are grown at identical temperatures and are more homogeneous resulting in a narrower emission. On the

contrary, for the heating cycle a faster rate is preferable, since the exact temperature values have less impact in the HT growth, the faster heating shortness the annealing time, minimizing Bi segregation/diffusion, and shortening the total recipe time by at least 30 minutes. All in all, from this subsection we can conclude that growth temperature is the most crucial parameter for the control and reproduction of emission energies, Additionally, using a low ramping rate low for the cooling cycle before the growth of bismide layers, helps to achieve narrower emissions.

4.4. Growth and Characterization of a Light Emitting Diode

In this subsection a bismide based LED device that was grown on AlAs sacrificial layer is discussed. The LED served as a proof of concept to demonstrate the emission from a bismide active region and to optimize the thickness of the sacrificial AlAs layer. The AlAs sacrificial layer was necessary for substrate removal. All the structures were grown on 350 µm thick GaAs substrates. 5x GaAsBi 5.5 nm thick RQWs, separated by 7 nm thick GaAs barriers were inserted between GaAs spacers. The active area was grown on 500 nm thick n-type GaAs:Si and covered with 500 nm thick p-type GaAs:Be (see Fig. 22). The carrier concentrations were chosen $2*10^{18}$ cm^{-3} for n-type and $5*10^{18}$ cm^{-3} for p-type. A part of the structure was etched down to n-type GaAs and In contacts were placed on doped layers to measure the EL of the LED.

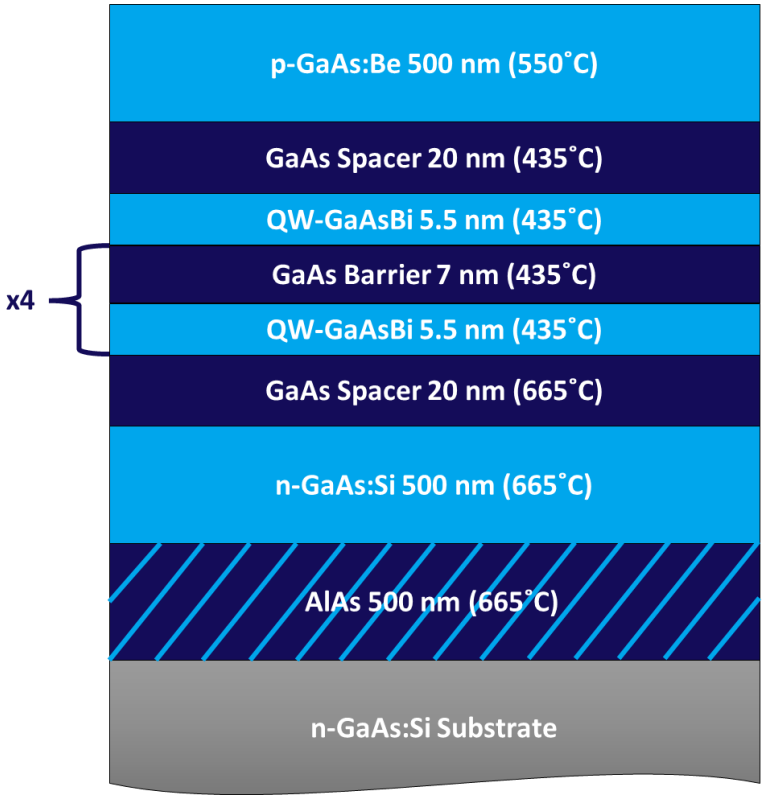

Fig. 22. GaAsBi 5xRQW LED structure. Temperatures provided from thermocouple readings.

The RTEL measurements (see Fig. 23) show luminescence at a peak wavelength of about 1.16ev (1070 nm), with stability for all excitation currents. Consequently, measurements were carried out with liquid nitrogen cooling at 80K, in this case the peak wavelength shifted to around 1.21 eV (1025 nm) at an excitation current of 60 mA. With decreasing injection currents, the emission experiences a red shift. This was also observed for a GaAsBi QW LED grown by *Richards et al.* and explained by the presence of localised states [24]. In lower temperature conditions holes fall into these localised states and do not have enough thermal energy to escape them. Since these states are situated within the band gap the emission energy is thus smaller than the band gap energy. With the increased injection current these localised states are being filled and the emission gradually shifts to shorter wavelengths.

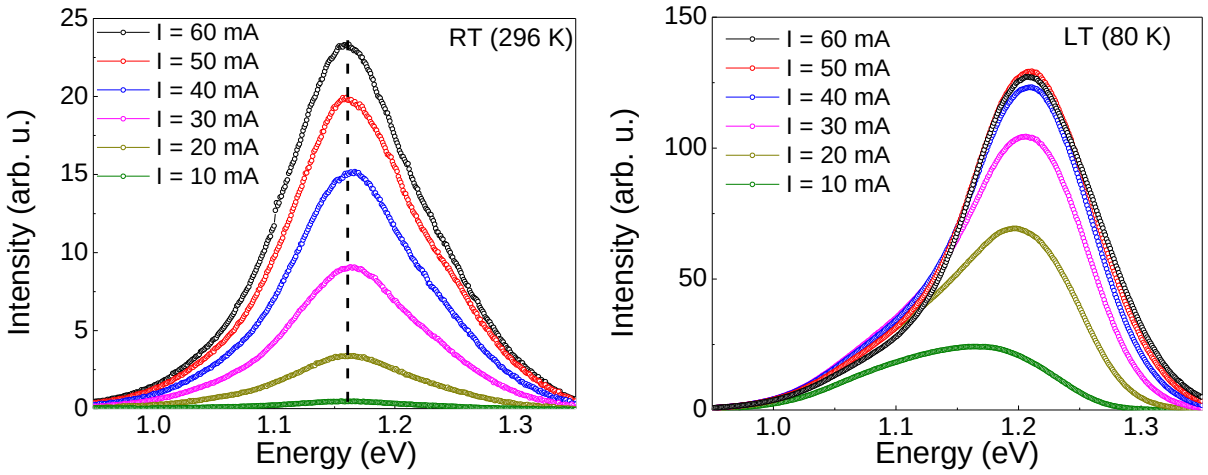

Fig. 23. Excitation dependent RTEL measurement for GaAsBi 5xRQW LED (dashed line serves as eye (guide).

Afterwards the attention was turned to finding the dominating carrier recombination mechanisms by plotting the integrated EL against the injection current on a double log scale. The slope of the results is an indication of the mechanism. In RT the slope is around 2, which is an indication of non-radiative recombination, by which the lower emission intensity is caused. At 80 K this slope is close to 1 which points to the radiative recombination being the dominant mechanism.

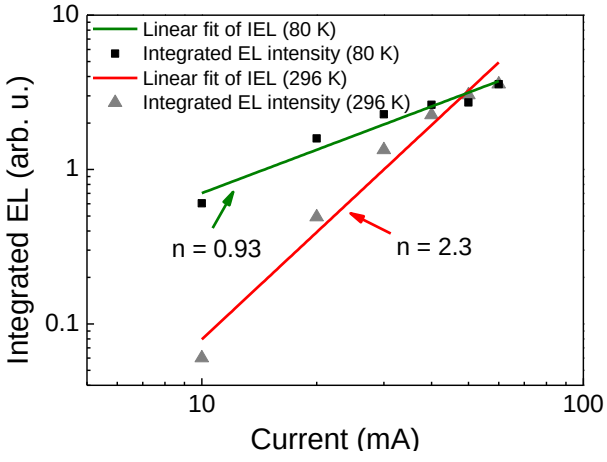

Fig. 24. Integrated EL intensity vs injection current at room temperature (grey triangles) and at 80 K (black squares).

Lastly, temperature dependence of the LED was investigated, the EL spectra and temperature dependence are given in Fig. 25.

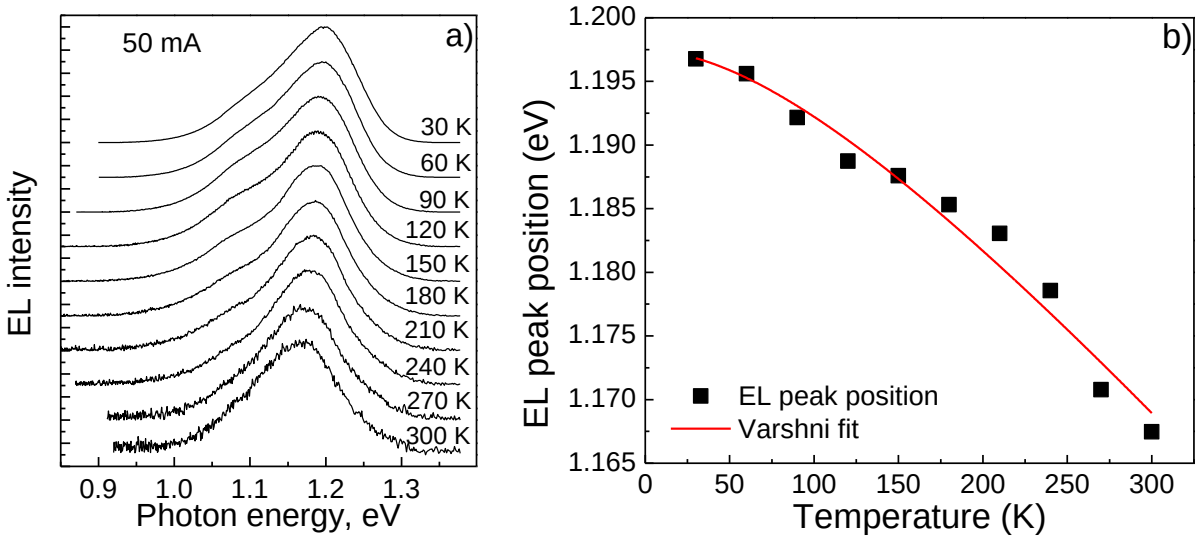

Fig. 25. a) Temperature dependent EL of the LED structure (at 50 mA injection current), and b) EL peak position dependence on temperature, fitted by a Vashni fit (red curve).

The results show appearance of a secondary EL peak that is mostly visible for spectra measured in the range of 90 K - 210 K. This is an indication that there are two radiative recombination paths in the structure. This is likely due to the non-uniformity of QWs (Bi content and dimensions) discussed in subsections 4.2. and 4.3. Nonetheless, the structure shows a very good temperature stability, which is important for device fabrication and is also an inherent advantage of GaAsBi. Through a temperature interval from 30 K to 300 K a difference of only 29 meV (27 nm) is observed. This is a great improvement from bulk GaAs band gap dependence, where in the same interval the difference would be 95meV (55 nm).

To conclude the LED structure shows good temperature stability and some localisation effects related with bismide materials. While a slight non-uniformity of the QWs is present, the dominant recombination mechanism at 80 K is radiative recombination, that is beaten by non-radiative recombination at room temperature.

4.5. Growth and Characterization of a Laser Diode

In this subsection a GaAsBi 3xRQW laser diode grown on AlAs sacrificial layer is discussed. The fabrication of the device followed a similar procedure to the LED growth. An optimal thickness of the AlAs sacrificial layer was chosen to be 1000 nm, to make the future removal of substrate easier. Then, a 1000 nm thick Si doped GaAs ($2*10^{18}$ cm^{-3}) contact layer was deposited (earlier lower thickness of 200 nm was tested, but it proved to be too thin for accurate etching). The active

region consists of 6.8 nm thick 3x GaAsBi RQWs separated by 7nm GaAs barriers and surrounded by two 25nm thick GaAs spacer layers. The active area was grown at low temperature (calibrated at 350 ˚C). Be and Si doped AlGaAs cladding ($5*10^{17}$ cm^{-3}) layers were grown for both charge transfer and waveguiding purposes. Finally the structure is capped with a p-type GaAs:Be contact layer with a carrier concentration of $5*10^{18}$ cm^{-3} (see sketch in Fig. 26 a). All n-type layers were grown at a usual HT growth temperature of 570 ˚C, while p-type regions were grown at 480 ˚C to ensure Be incorporation and minimise diffusion. Photolithography and etching procedures were carried out to form the laser bar and metallization. Metallization of contacts was done using electron beam, depositing Ti-Au on p-type and Au-Ge on n-type layer.

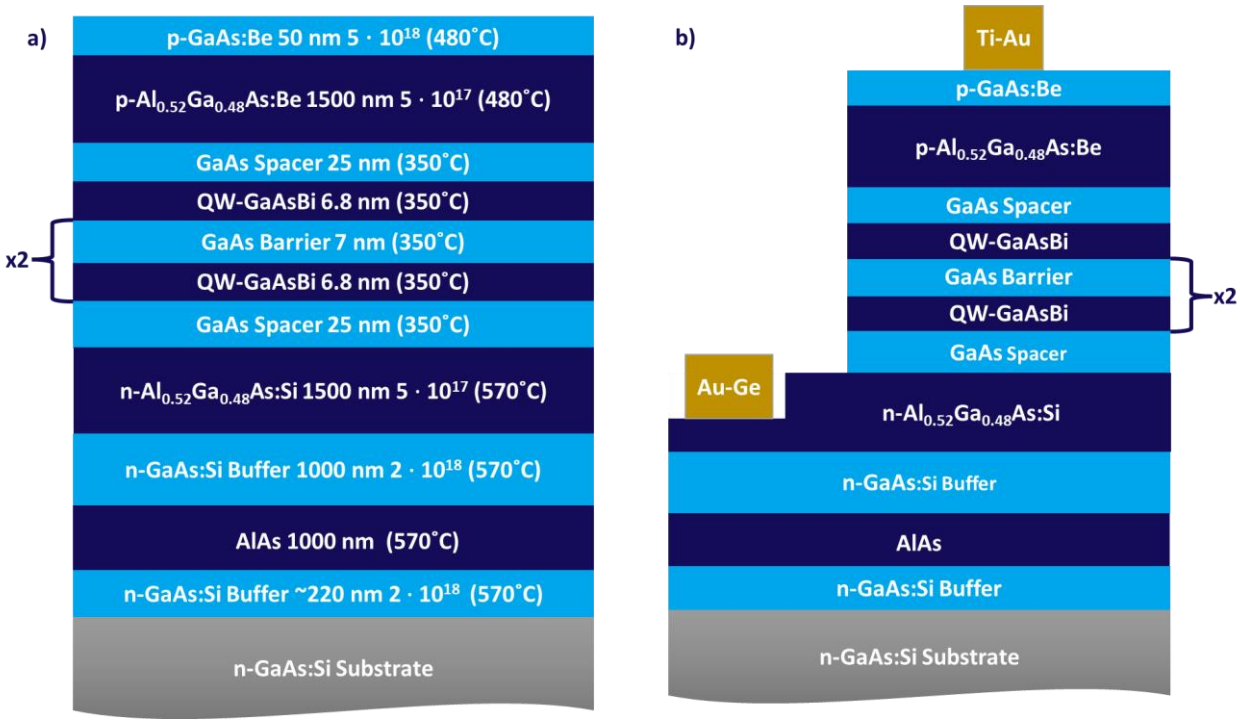

Fig. 26. a) 3xRQW GaAsBi LD structure. Growth temperatures and doping concentrations (in cm^{-3}) provided. b) Schematic of a laser bar after processing.

The LDs were cleaved to form the mirrors and tested using a pulsed bias at pulse duration of 15 to 200 ns and repetition rate of 1 kHz. At lower current EL from the structure was observed at a peak emission of 1.07 eV (see Fig 27), Increasing the current resulted in lasing demonstrated in Fig. 28. Lasing spectra were recorded at two temperatures 15 and 23 ˚C, the central emission was registered at 1.084 and 1.086 eV (1144 and 1142 nm) respectively, this constitutes a shift of 2 nm per 8 ˚C, again pointing to the good temperature stability of GaAsBi MQW based devices. It must be noted that the two lasing spectra were recorded at different monochromator slit widths, meaning that the emission intensity at 15 ˚C is substantially higher.

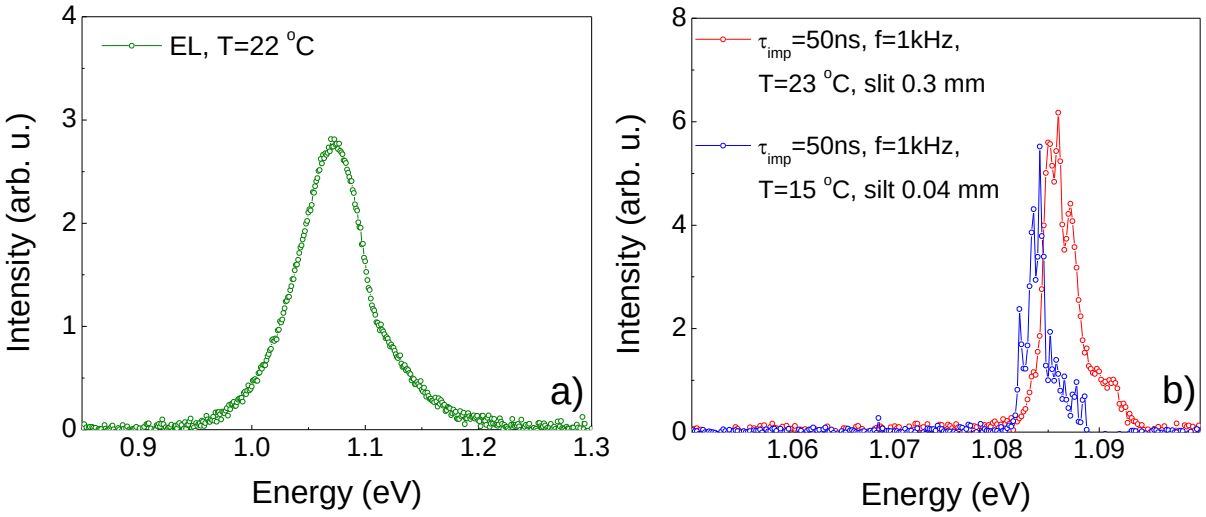

Fig. 27. a) EL spectrum of LD structure at room temperature. b) Lasing spectra of LD at room temperature (red) and at 15 ˚C (blue). Note that intensities of the spectra cannot be compared, since slit size was changed between measurements.

5. Conclusions

Technical Highlights:

- Multiple PL peak nature of grown MQW structures was determined to be influenced by growth temperature. It was found that high temperature capped structures exhibit worse uniformity of QWs: thickness and/or Bi distribution.
- The multiple peak problem was determined to be related to cooling and heating cycles. It was found that optimal ramping rate conditions for best QW uniformity are 5 ˚C/min for cooling and 25 ˚C/min for heating.

Technological Highlights:

- Atomic flux influence investigation determined that:
    - As:Ga ratio in the range from 0.8 to 1.21 does not shift the emission energy, though it can influence the overall emission intensity caused by a difference in crystalline and surface quality of the structures;
    - In the Bi flux range 1.43-3.35 * 10^{-7} Torr, the growth regime is not Bi limited, since the emission energy has no direct correlation with Bi flux. From this it is concluded that the Bi flux in this growth window is in excess of the maximum Bi incorporation threshold.
- Investigation of temperature influence on Bi content in GaAsBi QW, revealed that temperature is the main limiting factor in Bi incorporation. A bismide growth temperature of 350 ˚C was determined to be optimal for target emission at ~1.13 eV (1100 nm).
- An LED structure fabricated on AlAs sacrificial layer exhibited EL of about 1.16 eV (1070 nm) at room temperature and 1.21 eV (1025 nm) at 80 K. Integrated EL vs injection current plots reveal the dominant recombination mechanisms: non-radiative at room temperature, and radiative at 80 K.
- The LED showed good temperature stability with an emission change of 29 meV in the temperature range from 30 to 300 K.
- A Fabry-Perot type LD structure was fabricated on AlAs sacrificial layer and exhibited room temperature lasing at 1.084 eV (1142 nm). The device showed good temperature stability with a 2nm shift in emission, when cooled by 8 ˚C.

6. Santrauka

Artimosios infraraudonosios srities mikrolazerių aktyviosios terpės technologinių sąlygų optimizavimas

Aivaras Špokas

Šiame darbe aprašomas GaAsBi technologinių molekulinių pluštelių epitaksijos auginimo parametrų optimizavimas artimosios infraraudonosios srities šviestukams ir puslaidinikiniams lazeriams. Tiriant daugybines stačiakampes GaAsBi kvantines duobes buvo nustatyta, kad šiam darbui pasirinktuose auginimo rėžiuose dominuoja temperatūra limituotas augimo rėžimas. Atominių srautų įtakos tyrime nustatyta, kad srautai neturi įtakos emisijos energijai, tačiau turi įtakos struktūros kokybei ir emisijos intensyvumui. Temperatūros įtakos tyrimas atskleidė, kad būtent temperatūra yra pagrindinis parametras leidžiantis kontroliuoti emisijos bangos ilgį GaAsBi kvantinėse duobėse. Taip pat, šildymo ir šaldymo ciklų tyrimas parodė, kad lėtesnis šaldymas auginimo metu pagerina kvantinių duobių homogeniškumą, kuris nusako emisijos spektro linijos plotį. Atlikus techninio kalibravimo ir technologinių sąlygų optimizavimo procesus, bakalauriniame darbe buvo užaugintos dvi prietaisų struktūros, šviesą emituojantis diodas (LED) bei Fabry-Perot lazerinis diodas (LD). Abu prietaisai pasižymėjo bismidams būdingu temperatūriniu stabilumu. Darbe buvo įvertinti dominuojantys rekombinacijos mechanismai LED struktūrai. Šviesa emituojančio dijodo centrinė emisija kambario temperatūroje buvo užregistruota ties 1070 nm ir 1025 nm 80 K temperatūroje. Taip pat užregistruotas trijų GaAsBi kvantinių duobių pagrindu pagaminto LD spektras. Kambario temperatūroje, nustatytas lazerinės spinduliuotės bangos ilgis buvo ties 1144 nm.

7. References

[1] K. Oe and H. Okamoto, “New semiconductor alloy GaAs1-xBix grown by metal organic vapor phase epitaxy,” *Jpn. J. Appl. Phys., Part 2: Letters*, vol. 37, no. 11 PART A, pp. 1283–1285, 1998, doi: 10.1143/jjap.37.l1283.

[2] S. Francoeur, M. J. Seong, A. Mascarenhas, S. Tixier, M. Adamcyk, and T. Tiedje, “Band gap of GaAs1-xBix, 0<x< 3.6%,” *Appl. Phys. Lett.*, vol. 82, no. 22, pp. 3874–3876, Jun. 2003, doi: 10.1063/1.1581983.

[3] K. Alberi, O. D. Dubon, W. Walukiewicz, K. M. Yu, K. Bertulis, and A. Krotkus, “Valence band anticrossing in GaBi xAs 1-x,” *Appl. Phys. Let.t*, vol. 91, no. 5, pp. 10–13, 2007, doi: 10.1063/1.2768312.

[4] Y. Tominaga, K. Oe, and M. Yoshimoto, “Low temperature dependence of oscillation wavelength in GaAs1-x Bix laser by photo-pumping,” *Appl. Phys. Exp.*, vol. 3, no. 6, Jun. 2010, doi: 10.1143/APEX.3.062201.

[5] Weyers Markus, Sato Michio, and Ando Hiroaki, “Red Shift of Photoluminescence and Absorption in Dilute GaAsN Alloy Layers,” *Jpn. J. Appl. Phys.*, vol. 31, pp. 853–855, 1992, doi: 10.1143/JJAP.31.L853.

[6] Z. Batool *et al.*, “Bismuth-Containing III-V Semiconductors: Epitaxial Growth and Physical Properties,” *Molecular Beam Epitaxy: From Research to Mass Production*, pp. 139–158, 2012, doi: 10.1016/B978-0-12-387839-7.00007-5.

[7] W. Shan, W. Walukiewicz, J. W. Ager, III, E. E. Haller, J. F. Geisz, D. J. Friedman, J. M. Olson, and S. R. Kurtz, “Band Anticrossing in GaInNAs Alloys,” *Phys. Rev. Lett.* Vol. 82, no. 6, pp. 1221-1224, 1999, doi: 10.1103/PhysRevLett.82.1221

[8] I. P. Marko and S. J. Sweeney, “Progress Toward III-V Bismide Alloys for Near- and Midinfrared Laser Diodes,” *IEEE J. Sel. Top. Quantum Electron.*, vol. 23, no. 6, pp. 1-12, 2017, doi: 10.1109/JSTQE.2017.2719403.

[9] C. A. Broderick, M. Usman, S. J. Sweeney, and E. P. O’Reilly, “Band engineering in dilute nitride and bismide semiconductor lasers,” *Semicond. Sci. Technol.*, vol. 27, no. 9, 2012, doi: 10.1088/0268-1242/27/9/094011.

[10] R. D. Richards *et al.*, “Molecular beam epitaxy growth of GaAsBi using As2 and As 4,” *J. Cryst. Growth*, vol. 390, pp. 120–124, 2014, doi: 10.1016/j.jcrysgro.2013.12.008.

[11] R. B. Lewis, M. Masnadi-Shirazi, and T. Tiedje, “Growth of high Bi concentration GaAs 1-xBi x by molecular beam epitaxy,” *Appl. Phys. Lett.*, vol. 101, no. 8, pp. 1–5, 2012, doi: 10.1063/1.4748172.

[12] R. M. Feenstra, J. M. Woodall, and G. D. Pettit, "Observation of Bulk Defects by Scanning Tunneling Microscopy and Spectroscopy: Arsenic Antisite Defects in GaAs," *Phys. Rev. Lett.*, vol. 71, no. 8, pp. 1176-1179, 1993, doi: 10.1103/PhysRevLett.71.1176.

[13] J. Puustinen, J. Hilska, and M. Guina, "Analysis of GaAsBi growth regimes in high resolution with respect to As/Ga ratio using stationary MBE growth," *J. Cryst. Growth*, vol. 511, pp. 33–41, Apr. 2019, doi: 10.1016/j.jcrysgro.2019.01.010.

[14] B. A. Carter, V. Caro, L. Yue, C. R. Tait, and J. M. Millunchick, "The effect of III:V ratio on compositional and microstructural properties of GaAs1-xBix (0 0 1)," *J. Cryst. Growth*, vol. 548, Oct. 2020, doi: 10.1016/j.jcrysgro.2020.125815.

[15] T. B. O. Rockett *et al.*, "Influence of growth conditions on the structural and opto-electronic quality of GaAsBi," *J. Cryst. Growth*, vol. 477, pp. 139–143, 2017, doi: 10.1016/j.jcrysgro.2017.02.004.

[16] A. J. Ptak *et al.*, "Kinetically limited growth of GaAsBi by molecular-beam epitaxy," *J. Cryst. Growth*, vol. 338, no. 1, pp. 107–110, 2012, doi: 10.1016/j.jcrysgro.2011.10.040.

[17] M. Masnadi-Shirazi, D. A. Beaton, R. B. Lewis, X. Lu, and T. Tiedje, "Surface reconstructions during growth of GaAs 1-xBi x alloys by molecular beam epitaxy," *J. Cryst. Growth*, vol. 338, no. 1, pp. 80–84, 2012, doi: 10.1016/j.jcrysgro.2011.09.055.

[18] R. B. Lewis, D. A. Beaton, X. Lu, and T. Tiedje, "GaAs1 - x Bix light emitting diodes," *J. Cryst. Growth*, vol. 311, no. 7, pp. 1872–1875, 2009, doi: 10.1016/j.jcrysgro.2008.11.093.

[19] P. Ludewig *et al.*, "Electrical injection Ga(AsBi)/(AlGa)As single quantum well laser," *Appl. Phys. Lett.*, vol. 102, no. 24, pp. 1–4, 2013, doi: 10.1063/1.4811736.

[20] P. K. Patil *et al.*, "GaAsBi/GaAs multi-quantum well LED grown by molecular beam epitaxy using a two-substrate-temperature technique," *Nanotechnology*, vol. 28, no. 10, Feb. 2017, doi: 10.1088/1361-6528/aa596c.

[21] X. Liu *et al.*, "Continuous wave operation of GaAsBi microdisk lasers at room temperature with large wavelengths ranging from 127 to 141 μm," *Photonics Res.*, vol. 7, no. 5, p. 508, 2019, doi: 10.1364/prj.7.000508.

[22] J. E. Sinex, "Pulse Oximetry: Principles and Limitations," *Am. J. Emerg. Med.*, vol. 17, no. 1, pp. 59-66, 1999, doi: 10.1016/S0735-6757(99)90019-0.

[23] M. Ohring "The Material Science of Thin Films," *Academic Press*, 1992.

[24] R. D. Richards, C. J. Hunter, F. Bastiman, A. R. Mohmad, and J. P. R. David, "Telecommunication wavelength GaAsBi light emitting diodes," *IET Optoelectronics*, vol. 10, no. 2, pp. 34–38, Apr. 2016, doi: 10.1049/iet-opt.2015.0051.